Supporting Information

Thermoresponsive Scaffolds Fabricated Using Covalent Organic Frameworks for the Selective Removal of Water Contaminants

*Safoora Gazvineh[a], Mohammad Nemati[a], Siamak Beyranvand[a], Sara Saki[a], Kai Ludwig[b], Patrick Amsalem[c], Thorstenn Schultz[c,d], Chong Cheng[e], Mohsen Adeli[a,b]**

[a]*Faculty of Science, Department of Chemistry, Lorestan University, Khorramabad, Iran*

[b]*Forschungszentrum für Elektronenmikroskopie and Core Facility BioSupraMol, Institut für Chemie und Biochemie, Freie Universität Berlin, Fabeckstr. 36a, 14195 Berlin, Germany*

[c]*Institut für Physik, Humboldt-Universität zu Berlin, Newtonstr. 15, 12489 Berlin, Germany*

[d]*Helmholtz-Zentrum Berlin für Materialien und Energie GmbH, Berlin 14109, Germany*

[e]*College of Polymer Science and Engineering, State Key Laboratory of Polymer Materials Engineering, Sichuan University, Chengdu, 610065, China*

Corresponding author: adeli.m@lu.ac.ir (Mohsen Adeli), m.aadeli@fu-berlin.de (Mohsen Adeli)

Experimental

Materials and methods

1,4-benzenediboronic acid (96%), 2,3,6,7,10,11-hexahydroxytriphenylene (95%), N-isopropylacrylamide (97%), N, N′-methylenebis(acrylamide), α, ά-azobisisobutyronitrile, 1,4-dioxane (99.8%), mesitylene (98%), acetonitrile, tetrahydrofuran, toluene, methanol, acetone, hydrochloric acid were purchased from Merck and Sigma-Aldrich and used directly without further purification. The dialysis bag (Biotech Cellulose Ester) with (MWCO: 2 kDa and 14 kDa were purchased from Biotech Cellulose Ester Company) and used for purification of polymer. Polyurethane foam was purchased from Chemical plant in Alborz Industrial City, Iran.

Infrared spectra (FT-IR) were recorded in the solid-state using potassium bromide tablet preparation and Shimadzu-8500 S infrared spectrometer. TGA thermograms were recorded by a STA 409 apparatus (Linseis) in a temperature range of 30-800 ^{o}C with a heating rate of 10 ^{o}C/min under nitrogen gas. Elemental analysis was performed using ELEMENTAR device with detector columns for carbon, nitrogen, hydrogen and sulfur. Morphology of materials were investigated using scanning electron microscope (SEM) model LEO 440i under vacuum and at 10 Kv voltage. The device was equipped with an energy dispersive X-ray (EDX) microanalysis system that was capable of identifying the number of corresponding atomic elements in the compounds. Samples were dispersed in water and dropped on a silica holder. Then water was evaporated and samples were coated by a thin layer of gold. The X-ray diffraction (XRD) spectrum of compounds was recorded using a Halland Philips Xpert device (Cuk, radiation, λ=0.154056 nm) with a scanning speed of 2^{o}/min and in the range of 2θ = 80 - 10.

Transmission electron microscopy (TEM) images were recorded as below:

Carbon-coated collodium film covered copper grids (400 mesh) were hydrophilized by a 60 s glow discharging at 8 W in a BALTEC MED 020 device (Leica Microsystems, Wetzlar, Germany). Then 5 µl of the materials dispersion in water (0,01 mg/ml) was absorbed onto the hydrophilized grids. The supernatant fluid was removed by blotting with a filter paper and sample was allowed to dry in air. A standard holder was used to transfer the dried samples into a FEI Talos L120C transmission electron microscope (Thermo Fisher Scientific Inc., Waltham, Massachusetts, USA) equipped with a tungsten cathode. Images were taken with a 4k × 4k Ceta CMOS camera at a primary magnification of 36.000 x using an accelerating voltage of 120 kV.

X-ray photoelectron spectroscopy (XPS) was performed in an ultrahigh vacuum chamber (base pressure 5.10-10 mbar) using a JEOL JPS-9030 set-up comprising a photoelectron spectrometer hemispherical energy analyzer and a monochromatic Al Kα (hν = 1486.6 eV) X-ray source. The XPS measurements were performed with an energy resolution of ca. 0.9 eV as determined on a polycrystalline Ag 3d core level. During the XPS measurements, strong charging of the sample was noticed. For correcting this charging issue, the XPS spectra were rigidly shifted to lower binding energy so that the C 1s peak is positioned at 284.5 eV, a typical value for C-C bonds.[1]

Pseudo second order kinetics:

Pseudo-second order kinetics were investigated according to equation (4). The t/q_t diagram was drawn in terms of t for different concentrations of methylene blue, rhodamine B and fluorescein. Afterwards, the value of the correlation coefficient and the second-order pseudo-rate constants were calculated. Results are shown in the table S2.[2]

Results

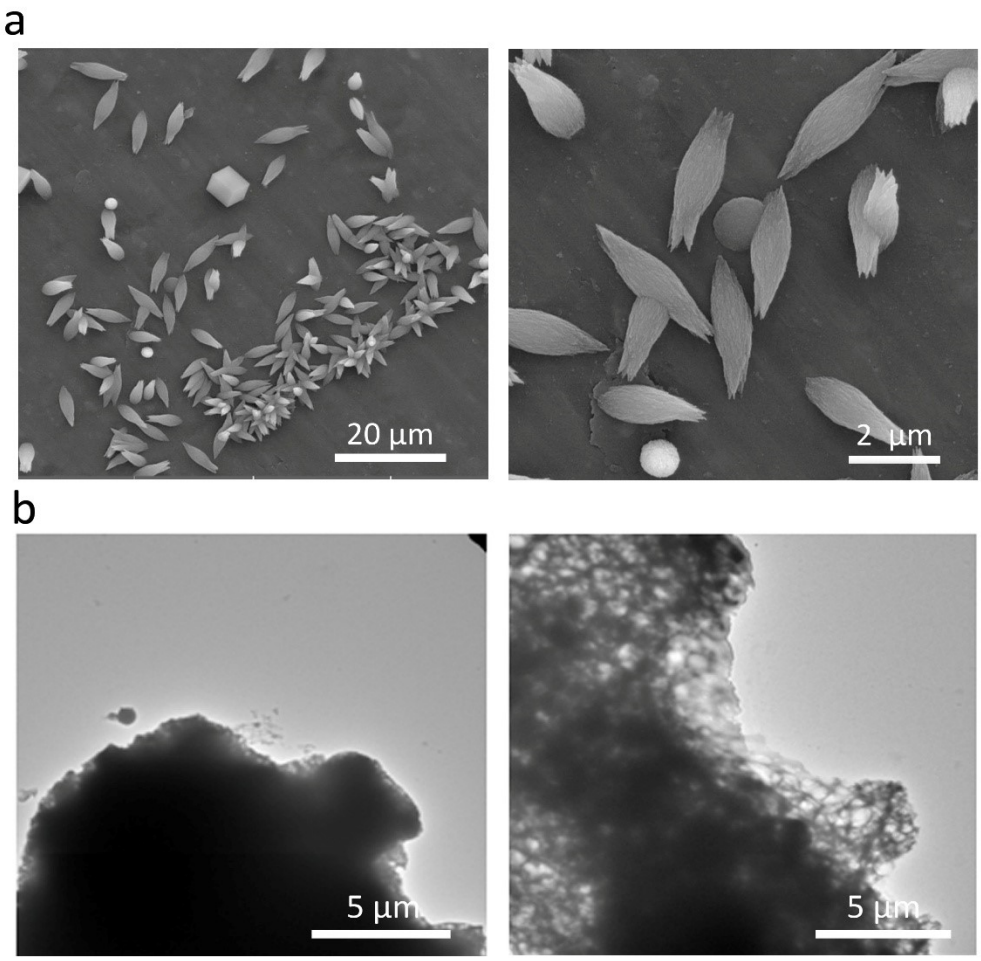

Figure S1. (a) SEM images of $PNIPAM_2$. (b) TEM images of PNIPAM1.

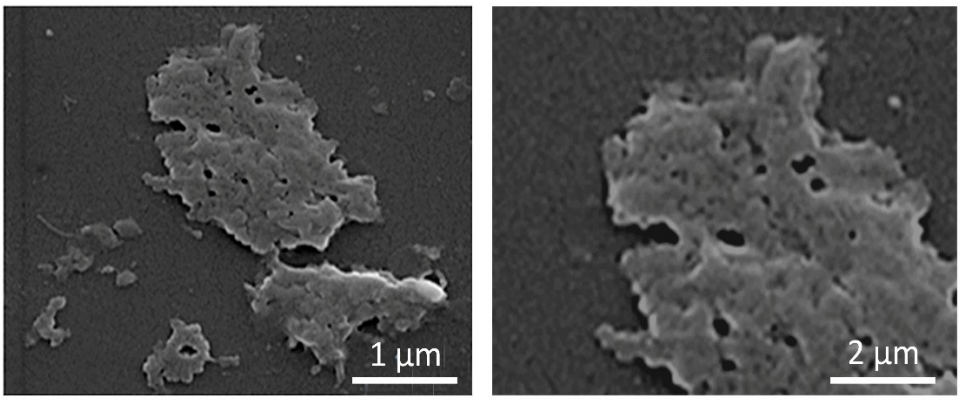

Figure S2. SEM images of 1 after 3 days incubation in acidic medium.

X-ray photoelectron spectroscopy (XPS) of **1**, **1**⊃PNIPAM and $PNIPAM_1$ were recorded (Figure S3a). Sample charging was observed during the measurements due to low conductivity of the materials, which was partly corrected by applying an energy shift in order to position the main C 1s peak at 284.5 eV. However, because of sample inhomogeneity, differential charging likely occurred, yielding additional artificial components in the XPS peaks, such as an unphysical C1s component at 281.5 eV for **1**⊃PNIPAM. Therefore, we stress that a precise assignment of the XPS results remains relatively involved but relevant aspects such as sample composition can still be discussed. XPS revealed that COF template was composed of carbon, oxygen and boron. The main peak component at 284.5 eV with a shoulder at 286.1 eV in the high resolution C1s spectrum were corresponding to the C=C and C-O bonds in the backbone of **1** (Figure S3a), respectively. For **1**⊃PNIPAM, an additional lower energy C1s component is observed, which is thought to be an artifact resulting from the charging correction procedure as differential charging occurs. The other two components are attributed to stem both from the COF and PNIPAM. For $PNIPAM_1$, C-C bond is observed at 284.5 eV and C=O / C-N bonds at 287.4 eV. N1s is only observed for **1**⊃PNIPAM and $PNIPAM_1$ at 399.2 eV and is readily absent for the COF, showing the inclusion of NIPAM in the COF structure. Boron is observed for **1** and **1**⊃PNIPAM, as expected. The double B 1s component for **1**⊃PNIPAM may be the result of an artifact of the charging correction procedure as also observed for the C1s of the same sample. Importantly, no B1s signal is detected in the $PNIPAM_1$ spectrum, which demonstrates the efficient removal of the COF by hydrolysis. The stoichiometries for the three samples are reported in Figure S3b and summarized in table S1.

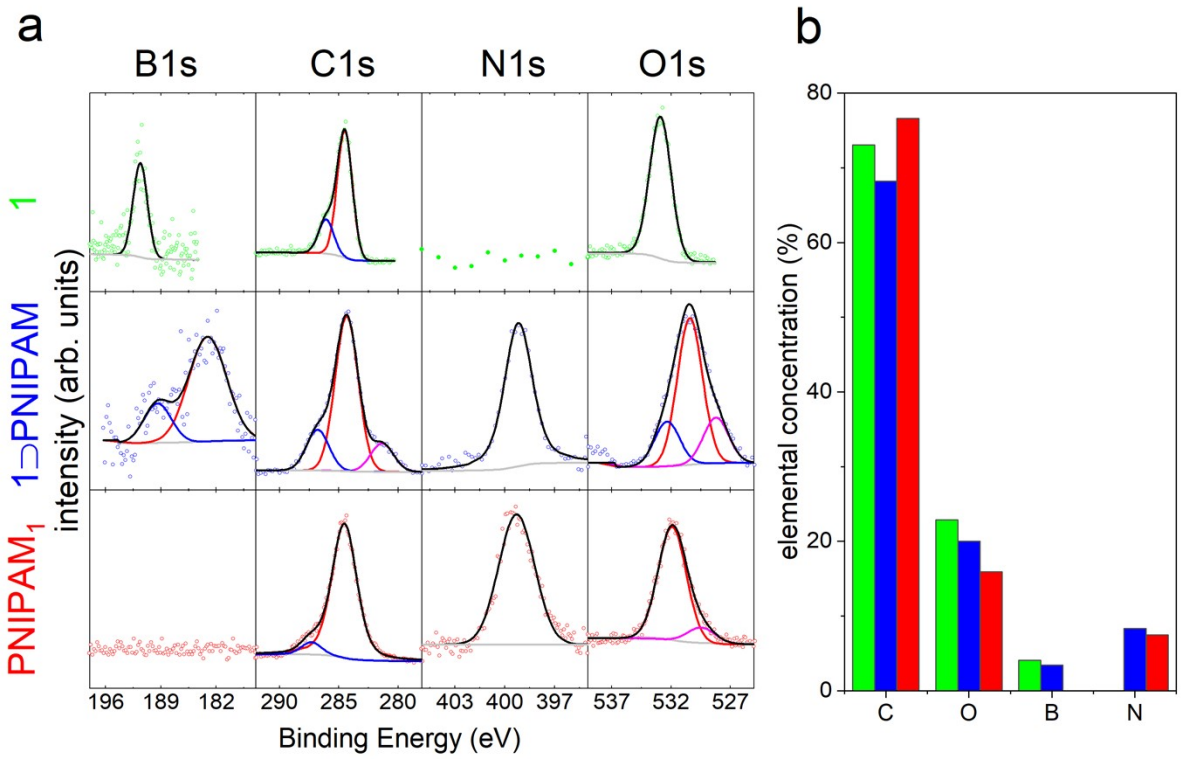

Figure S3. (a) Characterization of the synthesized materials by XPS. Highly resolved B1s, C1s, N1s and O1s XPS spectra of **1**, **1**⊃PNIPAM and $PNIPAM_1$. (b) Elemental concentration determined from the XPS spectra for each sample.

Table S1. Composition of 1, 1⊃PNIPAM and $PNIPAM_1$ based on EDX.

Element	C %	O %	N %	B %
1	73.1	22.9	-	4.0
1⊃PNIPAM	68.2	20.0	8.4	3.4
$PNIPAM_1$	77.6	16.0	7.4	-

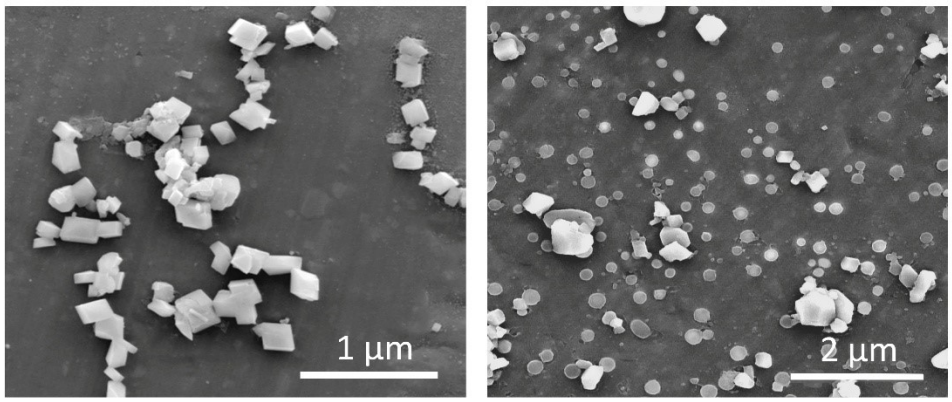

Figure S4. SEM images of $PNIPAM_1$ at 30 °C (left) and 39 °C (right).

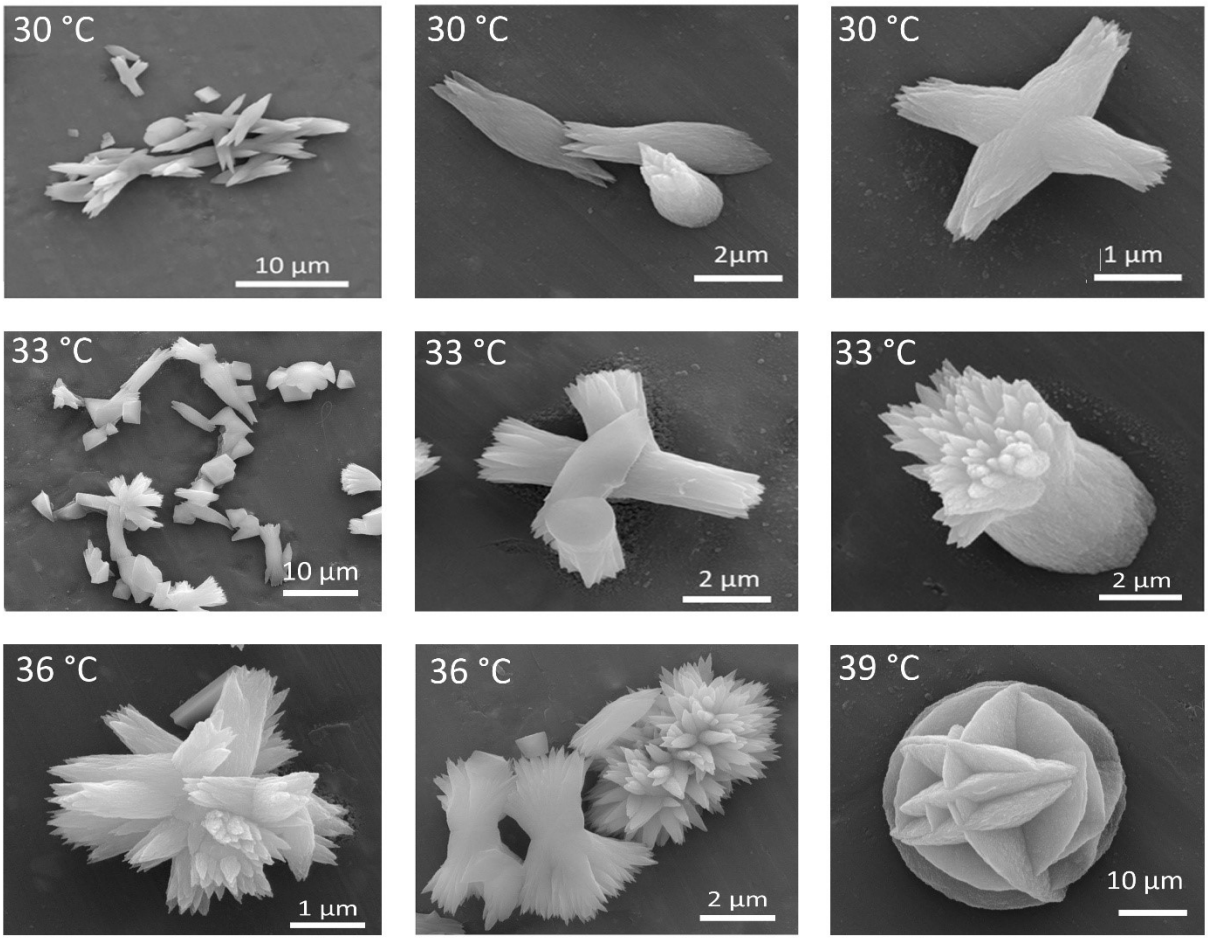

Figure S5. Changing the morphology of $PNIPAM_2$ from spindle-like microstructures to sunflower structures and globular networks, respectively, with increasing temperature from 30 °C to 39 °C.

Study of the kinetic of absorption of dyes by PNIPAM$_1$-sponge

In order to study the kinetic of absorption of dyes by PNIPAM$_1$-sponge, the absorption capacity q_t (mg.g^{-1}) and percentage of dye removal (%)R by the adsorbent at different time frames were calculated using equations (1) and (2), respectively:[3]

$$q_t = (C_0\text{-}C_t)\ V/m \qquad (1)$$

$$R\% = (C_0\text{-}C_t)/C_0 \times 100 \qquad (2)$$

where C_0 and C_t were the initial concentration (mg.L^{-1}) and concentration of dye (mg/l) at time t, V was the volume of the solution (L), and m was the mass of the adsorbent (g).

In order to understand the adsorption mechanism of dye, adsorption rate constants of pseudo-first and second order kinetic models for each dye were studied using equations (3) and (4) (Figure 5).

$$\ln(q_e - q_t) = \ln q_e - k_1 t \qquad (3)$$

$$t/q_t = 1/(k_2 q_e^2) + t/q_e \qquad (4)$$

K_1 and K_2 were the rate constants of the pseudo-first-order kinetic model (min^{-1}) and the pseudo-second-order kinetic model (g.mg^{-1}.min^{-1}) respectively, and t was absorption time (min). The values of the kinetic parameters are presented in table S2 and figure S6.

Table S2. Kinetic parameters of adsorption of different dyes by PNIPAM$_1$-sponge**.**

Adsorbent	C(mg/l)	First order kenetic			Second order kenetic		
		K_1	q_e	R^2	K_2	q_e	R^2
MB	5	0.0032	6.7593	0.9149	0.0010	7.2886	0.9121
	10	0.0030	5.8993	0.9353	0.0006	9.7656	0.7926
	20	0.0007	4.5405	0.4664	0.0016	8.0064	0.9739
Rh B	5	0.0041	2.0221	0.5935	0.0100	9.9404	0.9999
	10	0.0037	1.0085	0.9591	0.0009	17.6056	0.9976
	15	0.0021	5.4313	0.4069	0.6200	1.6129	0.9997
FL	5	0.0028	2.0068	0.4003	0.0014	7.1633	0.8040
	10	0.0147	5671.53	0.2687	0.0025	12.8700	0.9951
	15	0.0085	6.0618	0.0085	0.0049	20.5761	0.9998

Langmuir and Freundlich isotherms

Langmuir (5) and Freundlich (6) isotherms were also investigated to gain more information about kinetic of dye adsorption.

$$C_e/q_e = 1/K_l q_m + C_e/q_m \qquad (5)$$

$$\ln q_e = \ln K_f + 1/n \ln C_e \qquad (6)$$

where, Q_m was maximum adsorption capacity (mg. g^{-1}) and K_F and K_L were Freundlich and Langmuir constants, respectively.

Table S3. Different parameters for Langmuir and Freundlich isotherms for the absorption of MB, RhB and FL by $PNIPAM_1$-sponge.

Adsorbent	Langmuir Isotherm			Freundlich Isotherm			
	q_{max}	k_l	R^2	k_f	1/n	n	R^2
MB	3.6271	0.1936	0.9693	1.1105	0.3267	3.0609	0.9908
RhB	30.215	0.1597	1.0000	4.6440	0.6555	1.5260	0.9969
FL	15.1515	0.1909	0.9808	1.1200	1.0830	0.9234	0.9805

Table S4. R_L value for the adsorption of different concentrations of MB, RhB and FL by $PNIPAM_1$-sponge.

Adsorbent	C($mg.L^{-1}$)	R_L
MB	5	0.5081
	10	0.3406
	20	0.2052
RhB	5	0.5561
	10	0.3851
	15	0.2946
FL	5	0.5117
	10	0.3438
	15	0.2589

Table S5. Different parameters including removal efficiency, adsorption capacity and surface adsorption equilibrium constant for the adsorption of MB, RhB and FL by $PNIPAM_1$-sponge at 25 ^oC and 40 ^oC.

Adsorbent	T(°k)	k_{ad}	Ln k_{ad}	%R	$q_t(mg.g^{-1})$
MB	323	0.8030	-0.2194	44.5382	8.0037
	328	0.8479	-0.1650	45.8848	8.2457
	333	0.9134	-0.0906	47.7363	8.5784
	338	0.9543	-0.0468	48.8304	8.7750
	343	0.9575	-0.0434	48.9145	8.7902
Rh B	323	35.4230	3.5674	97.2545	16.9161
	328	34.2995	3.5351	97.1671	16.9010
	333	10.3194	2.3340	91.1656	15.8571
	338	4.9276	1.5949	83.1298	14.4593
	343	3.4716	1.2446	77.6369	13.5039
FL	323	21.4830	3.0673	95.5522	14.4757
	328	17.0705	2.8374	94.4661	14.3111
	333	10.5182	2.3531	91.3181	13.8342
	338	6.2369	1.8305	86.1819	13.0561
	343	5.3936	1.6852	84.3594	12.7800

Thermodynamic parameters

The values of equilibrium concentration (C_e) were obtained using the absorption value at different temperatures by equation 8.

$$K_{ad}=C_0-C_e/C_e \qquad (8)$$

Diagram of ln K_{ad} versus 1/T, provide parameters including ΔS/R and ΔH/R. Considering R=0.008314 ($kj.mol^{-1}.k^{-1}$), the values of ΔH (kj/mol) and ΔS ($kj.mol^{=1}.k^{-1}$) for surface absorption of MB, RhB and FL were calculated by equation 9.

$$Lnk_{ad}=\Delta S/R-\Delta H/RT \qquad (9)$$

Changes in Gibbs free energy (ΔG) for adsorption of MB, RhB and FL at different temperatures, were calculated using equation 10. The results are summarized in the table S6.

$$\Delta G^o=\Delta H^o-T\Delta S^o \qquad (10)$$

A negative ΔG indicates that the desired reaction is spontaneous. Positive ΔS indicates an increase in irregularity at the solid-liquid interface during the process of surface absorption on the

adsorbent. Positive ΔH indicated that adsorption is endothermic. Therefore, it is expected that the value of K_{ad} increases with increased temperature. Results in table S5 and S6 confirm this issue.

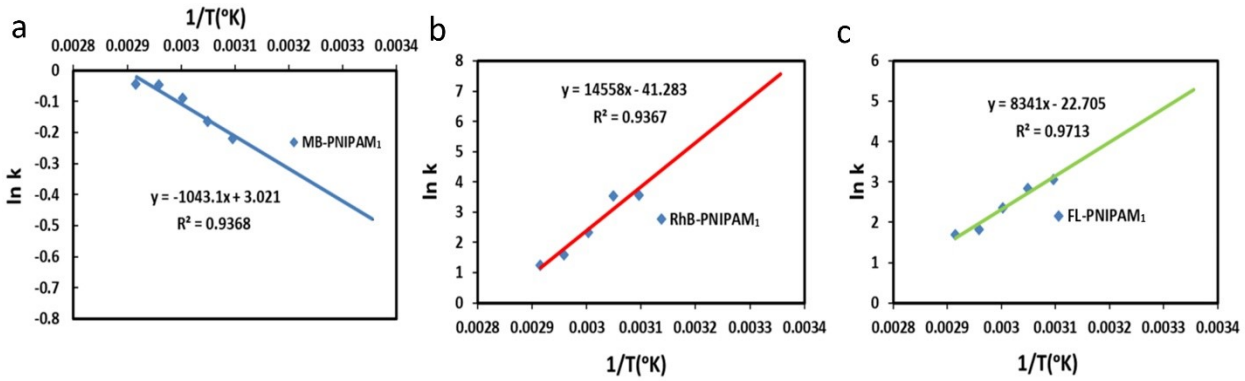

Figure S6. ln Kad versus 1/T for MB (a), RhB (b) and FL (c) at different temperatures.

Table S6. Thermodynamic parameters for the adsorption of MB, RhB and FL by $PNIPAM_1$-sponge.

Adsorbent	C(mg.L^{-1})	ΔH°(kj.mol^{-1})	ΔS°(j.mol^{-1}.k^{-1})	T(°k)	ΔG°(kj.mol^{-1})	R^2
MB	10	-8.6723	+0.0251	298	-16.1521	0.9368
				323	-16.7796	
				328	-16.9051	
				333	-17.0306	
				338	-17.1561	
				343	-17.2816	
Rh B	10	-121.0352	-0.3432	298	-18.7616	0.9367
				323	-10.1816	
				328	-8.4656	
				333	-6.7496	
				338	-5.0336	
				343	-3.3176	
FL	10	-69.3471	-0.1888	298	-13.0847	0.9713
				323	-8.3647	
				328	-7.4207	
				333	-6.4767	
				338	-5.5327	
				343	-4.5887	

Table S7. Adsorption capacity of $PNIPAM_1$-sponge to remove MB, RhB and FL from different samples of tap water. $PNIPAM_1$-sponge was incubated with dye solutions (5 ml, 50 ppm) for 24 hours without shaking at 25 °C and then the adsorption of dye was investigated using UV spectroscopy.

Absorbent	**Dyes (50 ppm)**	**Maximum dye adsorption ($mg.g^{-1}$)**
H_2o-Keeyow Lake Khorramabad	RhB	87.42
	FL	75.05
	MB	34.63
H_2o -Kakareza River Khorramabad	RhB	85.94
	FL	73.24
	MB	35.39
H_2o- Drinking water Khorramabad	RhB	89.51
	FL	63.93
	MB	35.50
D_2O	RhB	245
	FL	231
	MB	98

References

(1) Noda, Y.; Merschjann, C.; Tarábek, J.; Amsalem, P.; Koch, N.; Bojdys, M. J., Directional Charge Transport in Layered Two-Dimensional Triazine-Based Graphitic Carbon Nitride. *Angew. Chem. Int. Ed.* **2019,** *58* (28), 9394-9398.

(2) Li, Y.; Yang, C.-X.; Qian, H.-L.; Zhao, X.; Yan, X.-P., Carboxyl-functionalized covalent organic frameworks for the adsorption and removal of triphenylmethane dyes. *ACS Appl. Nano Mater.* **2019,** *2* (11), 7290-7298.

(3) Ghosh, I.; Kar, S.; Chatterjee, T.; Bar, N.; Das, S. K., Removal of methylene blue from aqueous solution using Lathyrus sativus husk: adsorption study, MPR and ANN modelling. *PSEP* **2021,** *149*, 345-361.